NUCLEAR CARDIOLOGY (V DILSIZIAN, SECTION EDITOR)

Advances in Digital PET Technology and Its Potential Impact on Myocardial Perfusion and Blood Flow Quantification

Fares Alahdab[1] · Mahmoud Al Rifai[1] · Ahmed Ibrahim Ahmed[1] · Mouaz H. Al-Mallah[1]

Abstract

Purpose of Review In this review, we explore the development of digital PET scanners and describe the mechanism by which they work. We dive into some technical details on what differentiates a digital PET from a conventional PET scanner and how such differences lead to better imaging characteristics. Additionally, we summarize the available evidence on the improvements in the images acquired by digital PET as well as the remaining pitfalls. Finally, we report the comparative studies available on how digital PET compares to conventional PET, particularly in the quantification of coronary blood flow.

Recent Findings The advent of digital PET offers high sensitivity and time-of-flight (TOF), which allow lower activity and scan times, with much less risk of detector saturation. This allows faster patient throughput, scanning more patients per generator, and acquiring more consistent image quality across patients. The higher sensitivity captures more of the potential artifacts, particularly motion-related ones, which presents a current challenge that still needs to be tackled.

Summary The digital silicon photomultiplier (SiPM) positron emission tomography (PET) machine has been an important development in the technological advancements of non-invasive nuclear cardiovascular imaging. It has enhanced the utility for PET myocardial perfusion imaging (MPI) and myocardial blood flow (MBF) quantification.

Keywords Positron emission tomography · Silicon photomultiplier · Myocardial blood flow · Coronary artery disease · Nuclear cardiology

Abbreviations

PET	Positron emission tomography
MPI	Myocardial perfusion imaging
MBF	Myocardial blood flow
SiPM	Silicon photomultiplier
TOF	Time of flight
CAD	Coronary artery disease
CMD	Coronary microvascular dysfunction
PMT	Photomultiplier tube
SPAD	Single-photon avalanche diode
DPC	Digital photon counter
FOV	Field of view
MFR	Myocardial blood flow reserve
MACE	Major adverse cardiovascular event

Introduction

The cardiologist's arsenal of diagnostic tests and evaluations for patients with possible coronary artery disease (CAD) grew over the years [1–3]. As a result, our understanding expanded not only of CAD but also of the limitations of such tools. One of the best non-invasive imaging modalities that emerged has been positron emission tomography (PET). It has offered advantages over several other modalities in terms of diagnostic accuracy, image quality, and lower radiation exposure to patients [3, 4]. Furthermore, PET myocardial perfusion imaging (MPI) has become routine when PET is considered for evaluating patients with chest pain [5, 6]. The use of PET MPI has evolved further into a gold standard for quantifying myocardial blood flow (MBF) to evaluate myocardial viability and coronary microvascular artery disease (CMD) [6–9]. It has also become an excellent diagnostic test for certain inflammatory conditions of the heart, such as sarcoidosis and endocarditis, as well as for infections associated with implanted medical devices, such as pacemakers and implanted heart valves [10–13]. Certain technological improvements over the years have directly enhanced the

utility of PET imaging as well as its image quality. Some of the developments were in the software used for the processing and analysis of images acquired by the PET scanners, while others were in the hardware of said scanners [14, 15]. One of the most recent improvements has been in the development of what is referred to as the "digital PET," where the advent of silicon photomultipliers (SiPM) has offered certain advantages to replace the analog glass-enclosed photomultiplier tubes (PMTs) [16] (Fig. 1).

Earlier versions of the SiPM detectors were introduced to medical imaging applications in 2004. They had the advantage of the smaller size and compatibility with magnetic resonance, but without the time of flight (TOF) capabilities [17–19]. Conventional PET scanners that involved pulses generated by multiple single-photon avalanche diode (SPAD) arrays required off-chip processing and anger-logic positioning decoding. However, since SiPM offered the ability for one SPAD to detect one scintillation photon, there was no more need for off-chip processing and anger logic decoding [20, 21]. The development of digital PET has improved image resolution as well as the signal-to-noise ratio. It also has the potential to reduce the radiation exposure to patients since smaller doses of the radiopharmaceuticals would need to be injected, while maintaining excellent image quality. In this review, we describe the technological improvements in digital PET imaging as well as the advantages of using it in

cardiovascular imaging. We also explore the pitfalls of using digital PET and the potential needed improvements. Finally, we summarize the available evidence on the prognostic utility of digital PET in cardiovascular imaging.

Technology Review: How Does Digital PET Work?

In PET/CT imaging, emitted gamma photos reach scintillation crystals, which in turn re-emit light photons that are directed to photomultiplier tubes (PMT) [22, 23]. PMTs are vacuum photo-tubes and are extremely sensitive detectors of light and multiply the current produced by incident light by as much as 100 million times producing voltage signals that are transformed into digital images using downstream electronic algorithms. PMTs have the advantage of high gain signal amplification, low noise, multichannel capabilities, and good timing performance. However, they have limited photon-to-electron quantum conversion efficiency and are relatively bulky.

Advances in PET/CT have resulted in the development of silicon photomultipliers (SiPMs) in lieu of PMTs [24, 25]. SiPMs are solid-state single-photon-sensitive devices that utilize single-photon avalanche diodes (SPAD) built on a common silicon substrate. The dimension of each single SPAD can vary from 10 to 100 μm, thereby decreasing detector size to 3 mm^2 (compared to 6 mm^2 with PMTs). In digital SiPMs, each SPAD is part of an array which operates as digital counter converting current signals to a digital bit of memory. Most digital PET scanners, however, use a hybrid (or analog) SiPMs where resistors are wired in parallel to get a readout of the total number of photons that are detected. These digital photon counters (DPC) have improved count rate sensitivity and can detect a dynamic range of photon detection down to a single scintillation photon. Current digital PET scanners use lutetium-based scintillation crystals directly coupled with individual SiPM DPC detectors (Table 1).

Compared to PMTs, SiPMs have improved light collection frequency with more efficient light collection. This results in improved energy and timing resolution. This also facilitates time of flight (TOF) measurements. During the process of positron annihilation, a pair of photons is released at 180 degrees opposite each other and reach the ring of detectors (coincidence detection). TOF measures not only the distance and attenuation of photons, but also the actual time difference (down to 6–200 picoseconds) between the detection of photons released during coincident events to more accurately identify the distance from the annihilation event to the detector. This translates to improved spatial resolution and better image quality. This also improves scanner sensitivity to detect ischemia, particularly subendocardial ischemia.
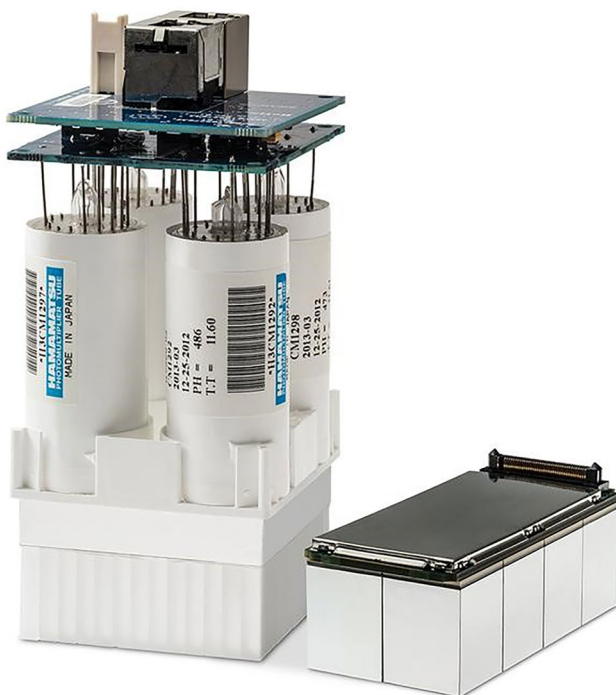

Fig. 1 Digital PET detector with 3.2-mm LSO crystals silicon photomultiplier (SiPM) on the **right**; analog photomultiplier tube (PMT) detector on the **left** (Unrestricted© Siemens Healthcare GmbH, 2017 MI-3710)

Table 1 Specifications comparison of three main digital PET scanners

|	Siemens healthineers biograph vision	GE discovery MI	Philips Vereos
Bore diameter	78 cm	60 cm	86 cm
CT rotation time	0.28 s	0.3	0.3 s
CT slices	64, 128	64, 128	64, 128
kVp	70–140	70–140	80–140
PET axial FOV	26.3 cm	15–25 cm	26.3 cm
Crystal size	$3.2 \times 3.2 \times 20$ mm	$3.95 \times 5.3 \times 25$ mm	$4 \times 4 \times 19$ mm
Effective sensitivity	100 cps/kBq	30 cps/kBq	23.4 cps/kBq
Time of flight performance	214 ps	377 ps	310 ps

Clinical Applications

From a historical perspective, the SiPMs were initially developed to be coupled with hybrid PET/CMR scanners. This can explain one of their advantages, namely being resistant to magnetism [26–28]. Their most important advantages, however, extend beyond that, particularly from a clinical applications perspective. In particular, the smaller sized SiPMs allow having one detector for each SiPM, thereby eliminating the need for anger-logic positioning decoding and tremendously improving the count rate performance of the PET scanner, contributing to the enhanced spatial resolution [25, 29, 30]. Furthermore, digital PET offers a considerably improved TOF temporal resolution, which leads to enhanced effective sensitivity allowing an improved image quality, a reduced patient radiation dose, and a faster image acquisition time. Enhanced TOF also improves the convergence of iterative reconstruction, image contrast, and image quality in patients with high BMI.

1. Improved image quality and signal to noise

Digital PET systems provide better image quality than their analog counterparts [31–33]. Improving the pixel count in the image acquired by a PET scan can be achieved by extending the time interval of image acquisition, by increasing the dose of the radiopharmaceutical, and by enhancing the detection efficiency of the PET machine. Digital PET achieves a higher count rate by the third method, all while substantially reducing the imaging time and the radiopharmaceutical dose injected (Fig. 2). In fact, a major advantage of digital PET scanners is their ultra-sensitivity and rapid image acquisition times [34, 35]. This is because the major leap in digital PET was in the dramatically improved TOF timing resolution [36–39]. While conventional analog PET scanners take several [4–7] minutes to capture the required image depending on the radiopharmaceutical used, digital PET scanners only take a few seconds. As each microcell in the detector can be individually activated, data processing takes place within each pixel on the silicon chip leading to rapid and accurate ultra-low-light photon counting. This also allows for high counting rates without detector saturation, as well as fast response enabling sub-nanosecond timing

Fig. 2 Signal-to-noise ratio: **a** a digital PET image (5 mCi FDG), **b** a conventional 3DPET image (20 mCi) of the same patient
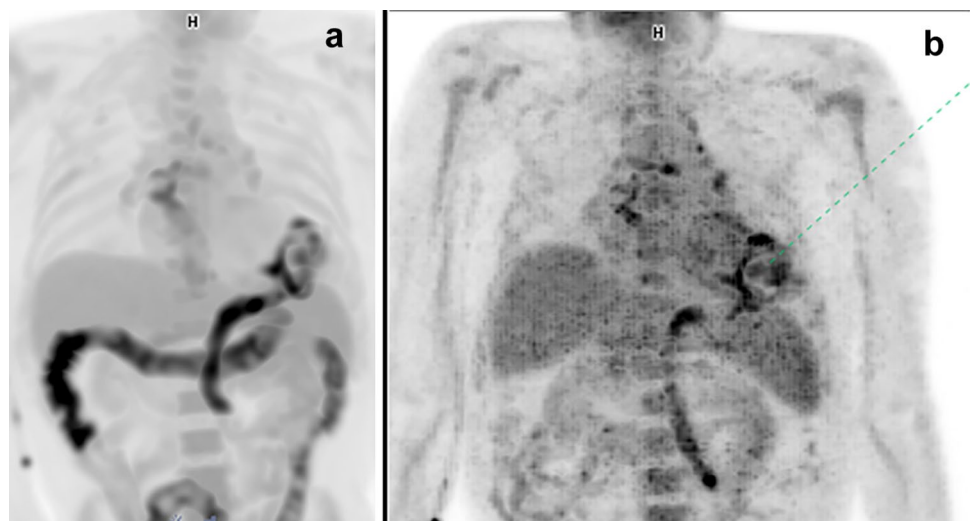
(300–400 ps), both of which would be critical for first-pass image acquisition [33, 38, 40, 41].

The high count rate accuracy is particularly important for MBF quantification [42•, 43•]. Van Dijk et al. conducted a comparative study evaluating the myocardial blood flow quantification by digital and conventional PET scanners [43•]. They compared the count rate performance of the digital and conventional PET systems using the dynamic range defined as the maximal measured activity. They chose Rubidium-82 (Rb-82) for its short half-life (76 s) and compared the dynamic ranges yielded by the three different PET machines included (a digital PET prototype system from Philips, an Ingenuity TF from Philips, and a Discovery 690 from GE). They noted that absolute activity bias increased for all three scanners with increasing activity, but the digital PET prototype system suffered the least increase. Therefore, the count rate performance of the digital PET prototype was less affected at higher activities, and the applied dead time correction was considerably lower than in the conventional PET systems. They noted that this may present the opportunity for further corrections to improve the dynamic range of the digital PET scanner. Continued improvement in count rates as well as effective sensitivity would be expected to enhance the precision and reliability of MBF assessment by digital PET.

The background noise, defined as dark count rates, is processed within each individual counter effectively. The digital PET scanner operates by allowing each sensor to function independently. When only the sensors that have received sufficient photons above a certain threshold are activated, while those that did not meet the preconfigured threshold are deactivated, the nosiest cells (i.e., those with high dark count rates) are switched off [25]. The result is a much better signal-to-noise ratio.

2. Reduction in the injected radiopharmaceutical dose

A more efficient light photon collection method and higher effective time rates allows smaller crystals and lesser doses of the radiotracer to be used. Less ionizing radiation can also decrease the likelihood of crystal saturation, especially during the initial acquisition phases of the scanning protocol. The improved TOF with digital PET allows for yielding higher sensitivity with the ability to use a reduced dose of the isotope injected, as compared to conventional PET scanners [25]. One additional factor contributing to a lower dose of the radiopharmaceutical is the expanded axial field of view (FOV) of many of the digital PET scanners available for cardiovascular imaging [44]. An expanded axial FOV also reduces the time necessary for undergoing the imaging process [45]. The end results are lower stressor dose needed, lower patient radioisotope needed, lower elution volume, and a more efficient generator usage as it ages. All

leads to a better patient experience as well as faster patient throughput.

Some labs with access to this technology have reduced their radiopharmaceutical injected dose significantly, while maintaining image acquisition time. For example, for Rubidium-82, 50–60 mci are injected when utilizing 2 cameras. This can be reduced to 25–30 mci with 3D systems and to 10–20 mci when utilizing digital PET scanners (Fig. 3).

In addition, detector saturation rarely occurs in these systems. Phantom experiments showed that saturation with Rubidium-82 occurs at 60 mci, a dose which is not used in clinical practice while utilizing these systems.

Potential Artifacts

As the sensitivity, TOF temporal resolution, and spatial resolution are higher for the SiPM PET scanner, the image quality becomes more sensitive to the artifacts, particularly those resulting from motion [42•]. The more apparent degrading influence of motion then requires even more need for correction. Motion blurring may lead to major artifacts in perfusion imaging. Artifacts stemming from motion tend to hamper image interpretation and may render PET scans as non-diagnostic, or worse, incorrectly interpreted. This emphasizes the need for continued advancement in multidimensional motion correction relating to both the heart movement as well as breathing [46]. Luckily, digital PET scanners enable data-driven motion correction where motion is ameliorated from the acquired raw images [47••] (Fig. 4).

Another potential artifact with digital PET stems from the improved spatial resolution as it exaggerates the appearance of apical thinning (Fig. 5).

Prognostic Value in Prior Studies

Few published studies have looked at the prognostic role of digital PET. Two prior studies were published from the Lausanne University Hospital in Switzerland. Dietz and colleagues assessed the prognostic role of digital silicon photomultiplier (SiPM) PET in 234 consecutive patients with suspected ischemia and followed over a median of 652 days for incident MACE (major adverse cardiovascular events: a composite of cardiac death, myocardial infarction, percutaneous coronary intervention (PCI)/coronary artery bypass graft (CABG) > 6 months post-imaging, hospitalization for heart failure or new onset stable angina) [48]. The authors evaluated global and minimum regional values for stress myocardial blood flow (MBF), myocardial flow reserve (MFR), and the myocardial flow capacity radius (MFC radius—the square root of the sum of stress MBF and MFR squared). This was a predominantly male (65%)
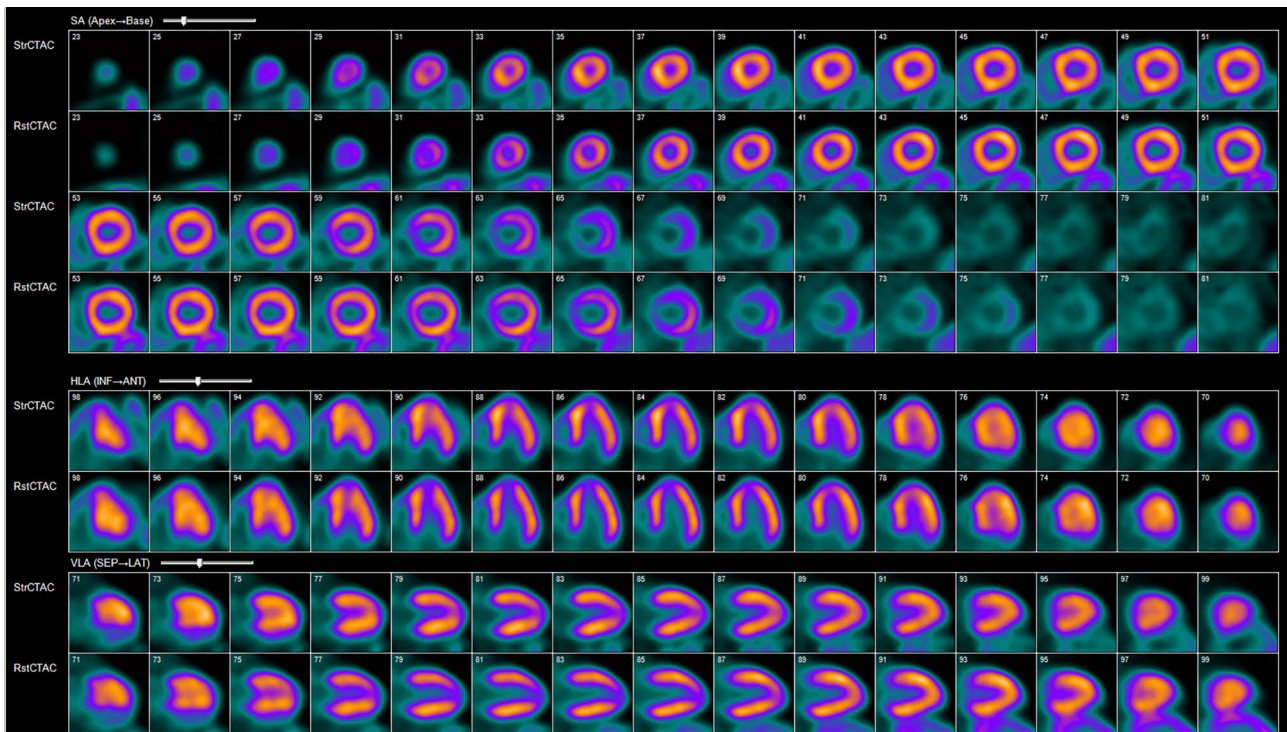
Fig. 3 A digital PET image of a patient with a BMI of 46 and a Rb-82 injection dose of 10 mCi. This was a 72-year-old female patient with DM type-2 who had presented with recurrent syncopal episodes, hypotension, and generalized weakness. Her cardiac PET scan showed a normal perfusion with a normal global myocardial blood flow reserve (2.2) and a coronary artery calcium score of 14

older cohort (median age 72 years) with a high burden of known CAD and cardiovascular risk factors (54% known CAD, 73% hypertension, 36% diabetes, 68% dyslipidemia). A total of 47 participants experienced MACE during the follow-up period. Patients experiencing MACE had similar resting MBF, but significantly lower global and regional minimum stress MBF, MFR, and MFC radius. The receiver operator characteristics analysis found regional stress MBF of 1.94/1.7, MFR of 1.98/1.75, and MFC radius of 3.12/2.7 global/minimum regional values, respectively, achieved the ideal balance of sensitivity and specificity in identifying patients with MACE. These thresholds were significantly associated with the incident event in both univariable and multivariable cox regression models. In addition, the authors showed that MFC was incrementally prognostic over MFR and stress MBF.

More recently, the same group has also published an abstract at the Annual Congress of the European Association
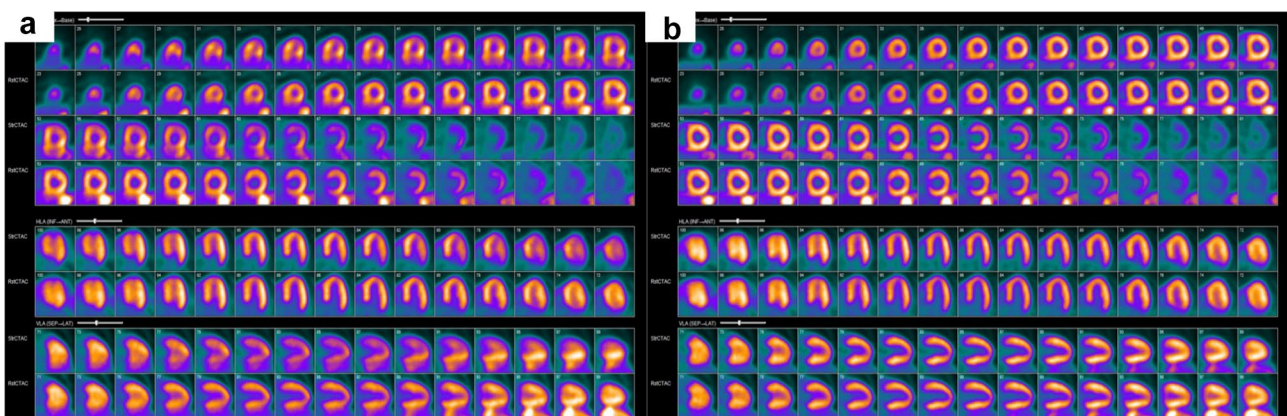

Fig. 4 Data-driven motion correction (DDMC): **a** before, **b** after motion correction
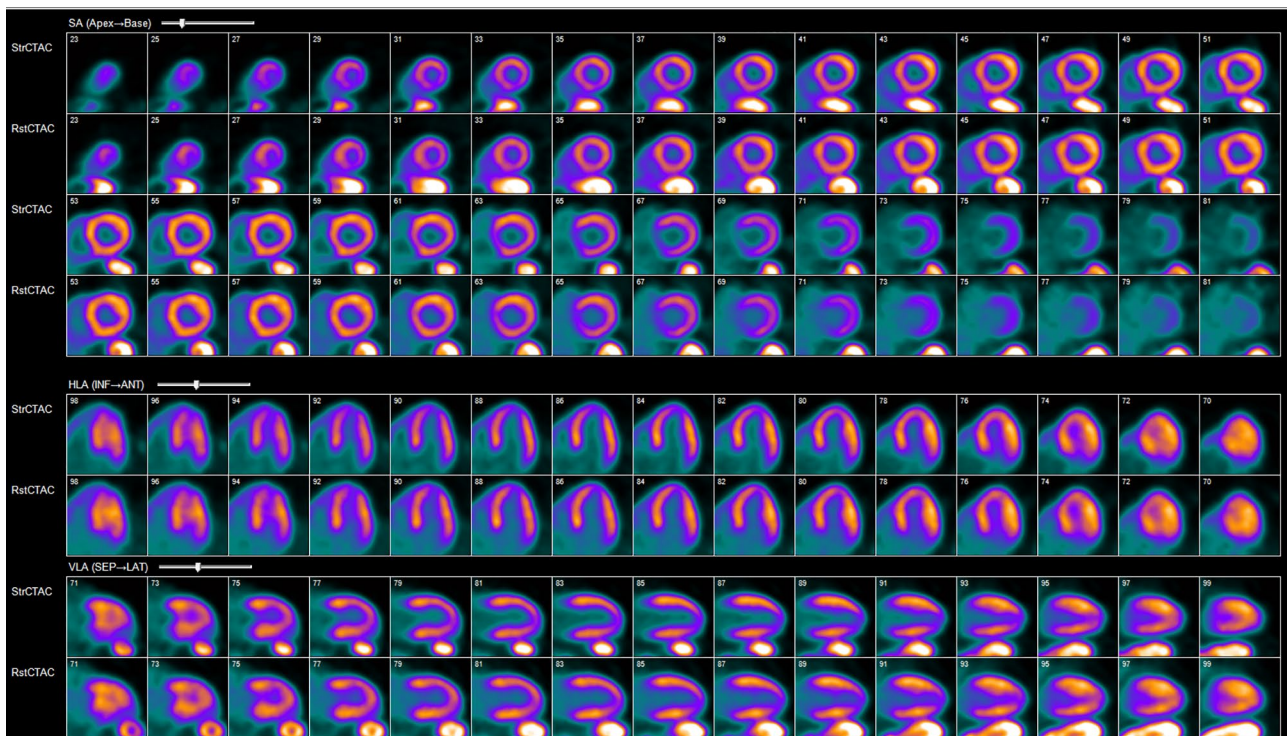
Fig. 5 A digital PET scan showing apical thinning. This was for a 64-year-old male patient with past medical history of CAD, hypertension, and hyperlipidemia. He had presented with chest pain. His car-diac PET scan showed a normal perfusion study, a borderline normal MBF (1.9), and apical thinning was noted on the digital PET scan

of Nuclear Medicine. Here, the authors aimed to compare the prognostic value of regional MFC to global stress MBF and MFR [49]. Although all 3 were independently associated with incident MACE in multivariable models adjusted for clinical factors, only stress MBF was associated with the outcome in multivariable models with all 3 metrics.

The largest study on the prognostic role of digital PET is that of Ahmed and Al Rifai et al. on 3678 patients with known or suspected CAD who were prospectively enrolled at the Houston Methodist DeBakey Heart and Vascular Center in Houston, Texas [50••]. Similar to the previous study, the cohort was composed of older patients (mean age 67 years, 52% men) with a burden of cardiovascular comorbidities and attendant known CAD (55% hypertension, 42% dyslipidemia, 32% diabetes, and 25% prior CAD). During a median follow-up of 8.5 (3.0–15.4) months, 229 patients experienced the primary outcome (all-cause death, myocardial infarction, and revascularization > 90 days after PET imaging). In multivariable models adjusting for traditional risk factors and relative PET perfusion variables, the authors showed that an impaired MFR (MFR < 2) was significantly associated with incident events. Furthermore, accounting for MFR improved model discrimination and risk reclassification. The aforementioned studies were all done using the

Biograph Vision PET/CT scanner (Siemens Healthineers, Knoxville, TN, USA). Biograph Vision 600 has an axial FOV of 26.3 cm, a TOF performance of 214 ps, a sensitivity of 16, and an effective sensitivity of 79.1. MBF was also quantified using the one compartment model of rubidium kinetics as described by Lortie [51].

Conclusion

Overall, digital PET has been a great development in the technological advancements of non-invasive cardiovascular imaging modalities. It has offered superb utility for myocardial perfusion imaging and MBF quantification. Its high sensitivity and TOF allow lower activity and scan times, with much less risk of detector saturation. This allows faster patient throughput, scanning more patients per generator, and acquiring more consistent image quality across patients. The higher sensitivity captures more of the potential artifacts, particularly motion-related ones, which presents a challenge that still needs to be tackled. Data-driven motion correction, as well as machine learning motion correction, may prove helpful in that regard.

Key Points

- Digital PET has been an important advancement in non-invasive cardiovascular imaging, particularly for quantification of myocardial perfusion imaging.
- Silicon photomultipliers in digital PET have offered substantial improvements in several aspects of PET image acquirement, leading to higher sensitivity.
- Further improvement in motion correction is still needed to optimize the quality of digital PET images.

Compliance with Ethical Standards

Conflict of Interest Dr. Al-Mallah discloses research funding from Siemens and acts as a consultant to Jubilant. The rest of the authors have nothing to disclose.

Human and Animal Rights and Informed Consent This article does not contain any studies with human or animal subjects performed by any of the authors.

References

Papers of particular interest, published recently, have been highlighted as:
- Of importance
- ● Of major importance

1. Al-Mallah MH, Sitek A, Moore SC, Di Carli M, Dorbala S. Assessment of myocardial perfusion and function with PET and PET/CT. J Nucl Cardiol. 2010;17:498–513.
2. El-Tallawi KC, Aljizeeri A, Nabi F, Al-Mallah MH. Myocardial perfusion imaging using positron emission tomography. Methodist Debakey Cardiovasc J. 2020;16:114–21.
3. Khalaf S, Chamsi-Pasha M, Al-Mallah MH. Assessment of myocardial viability by PET. Curr Opin Cardiol. 2019;34:466–72.
4. Case JA, deKemp RA, Slomka PJ, Smith MF, Heller GV, Cerqueira MD. Status of cardiovascular PET radiation exposure and strategies for reduction: an information statement from the cardiovascular PET Task Force. J Nucl Cardiol. 2017;24:1427–39.
5. Bateman TM, Dilsizian V, Beanlands RS, DePuey EG, Heller GV, Wolinsky DA. American Society of Nuclear Cardiology and Society of Nuclear Medicine and Molecular Imaging Joint Position Statement on the Clinical Indications for Myocardial Perfusion PET. J Nucl Cardiol. 2016;23:1227–31.
6. Ziadi MC, Dekemp RA, Williams K, et al. Does quantification of myocardial flow reserve using rubidium-82 positron emission tomography facilitate detection of multivessel coronary artery disease? J Nucl Cardiol. 2012;19:670–80.
7. Murthy VL, Bateman TM, Beanlands RS, et al. Clinical quantification of myocardial blood flow using PET: joint position paper of the SNMMI Cardiovascular Council and the ASNC. J Nucl Med. 2018;59:273–93.
8. Murthy VL, Naya M, Foster CR, et al. Improved cardiac risk assessment with noninvasive measures of coronary flow reserve. Circulation. 2011;124:2215–24.
9. Schindler TH. Myocardial perfusion PET for detection and reporting of coronary microvascular dysfunction: a consensus expert panel statement. J Am Coll Cardiol Img 2023.
10. Doherty JU, Kort S, Mehran R, Schoenhagen P, Soman P. ACC/AATS/AHA/ASE/ASNC/HRS/SCAI/SCCT/SCMR/STS 2017 Appropriate Use Criteria for Multimodality Imaging in Valvular Heart Disease: A Report of the American College of Cardiology Appropriate Use Criteria Task Force, American Association for Thoracic Surgery, American Heart Association, American Society of Echocardiography, American Society of Nuclear Cardiology, Heart Rhythm Society, Society for Cardiovascular Angiography and Interventions, Society of Cardiovascular Computed Tomography, Society for Cardiovascular Magnetic Resonance, and Society of Thoracic Surgeons. J Am Coll Cardiol. 2017;70:1647–72.
11. Tarkin JM, Chen W, Dweck MR, Dilsizian V. Molecular imaging of valvular diseases and cardiac device infection. Circ Cardiovasc Imaging. 2023;16: e014652.
12. Dilsizian V, Budde RPJ, Chen W, Mankad SV, Lindner JR, Nieman K. Best practices for imaging cardiac device-related infections and endocarditis: a JACC: Cardiovascular Imaging Expert Panel Statement. JACC Cardiovasc Imaging. 2022;15:891–911.
13. Kim J, Feller ED, Chen W, Liang Y, Dilsizian V. FDG PET/CT for early detection and localization of left ventricular assist device infection: impact on patient management and outcome. JACC Cardiovasc Imaging. 2019;12:722–9.
14. Tahari AK, Lee A, Rajaram M, et al. Absolute myocardial flow quantification with (82)Rb PET/CT: comparison of different software packages and methods. Eur J Nucl Med Mol Imaging. 2014;41:126–35.
15. Nesterov SV, Deshayes E, Sciagra R, et al. Quantification of myocardial blood flow in absolute terms using (82)Rb PET imaging: the RUBY-10 Study. JACC Cardiovasc Imaging. 2014;7:1119–27.
16. Renker D. New trends on photodetectors. Nucl Instrum Methods Phys Res, Sect A. 2007;571:1–6.
17. Lewellen TK. Recent developments in PET detector technology. Phys Med Biol. 2008;53:R287-317.
18. Catana C, Wu Y, Judenhofer MS, Qi J, Pichler BJ, Cherry SR. Simultaneous acquisition of multislice PET and MR images: initial results with a MR-compatible PET scanner. J Nucl Med. 2006;47:1968–76.
19. Vandenberghe S, Mikhaylova E, D'Hoe E, Mollet P, Karp JS. Recent developments in time-of-flight PET. EJNMMI Phys. 2016;3:3.
20. Frach T, Prescher G, Degenhardt C, De Gruyter R, Schmitz A, Ballizany R. The digital silicon photomultiplier — principle of operation and intrinsic detector performance. 2009 IEEE Nuclear Science Symposium Conference Record (NSS/MIC). 2009.
21. Wagatsuma K, Miwa K, Sakata M, et al. Comparison between new-generation SiPM-based and conventional PMT-based TOF-PET/CT. Phys Med. 2017;42:203–10.
22. Mirzoyan R, Laatiaoui M, Teshima M. Very high quantum efficiency PMTs with bialkali photo-cathode. Nuclear Instruments and Methods in Physics Research Section A: Accelerators, Spectrometers, Detectors and Associated Equipment. 2006;A:230–232.
23. Roncali E, Cherry SR. Application of silicon photomultipliers to positron emission tomography. Ann Biomed Eng. 2011;39:1358–77.
24. Bondarenko G, Buzhan P, Dolgoshein B, Golovin V, Guschin E, Ilyin A, et al. Popova, K. Smirnov. Limited Geiger-mode micro-cell silicon photodiode: new results. Nuclear Instruments and Methods in Physics Research Section A: Accelerators, Spectrometers, Detectors and Associated Equipment. 187–192.
25. Zhang J, Maniawski P, Knopp MV. Performance evaluation of the next generation solid-state digital photon counting PET/CT system. EJNMMI Res. 2018;8:97.

26. Hughes PJ, Herbert D, Stewart A, Jackson JC. Tiled silicon photomultipliers for large-area low-light sensing applications. Proc SPIE-Int Soc Opt Eng. 2007.

27. Stewart AG, Greene-O'Sullivan E, Herbert DJ, Saveliev V, Quinlan F, Wall L, Hughes PJ, Mathewson A, Jackson JC. Study of the properties of new SPM detectors. Proc SPIE-Int Soc Opt Eng. 2006;6119:1–10.

28. Espana S, Tapias G, Fraile LM, Herraiz JL, Vicente E, Udias J, et al. Performance evaluation of SiPM detectors for PET imaging in the presence of magnetic fields. IEEE Nucl Sci Symp Conf Rec. 2008:M02–4.

29. Schaart DR, Charbon E, Frach T, Schulz V. Schulz. Advances in digital SiPMs and their application in biomedical imaging. Nuclear Instruments & Methods in Physics Research Section Accelerators, Spectrometers, Detectors and Associated Equipment. 2016;48:31–52.

30. Baratto L, Park SY, Hatami N, et al. 18F-FDG silicon photomultiplier PET/CT: A pilot study comparing semi-quantitative measurements with standard PET/CT. PLoS ONE. 2017;12: e0178936.

31. Nguyen NC, Vercher-Conejero JL, Sattar A, et al. Image quality and diagnostic performance of a digital PET prototype in patients with oncologic diseases: initial experience and comparison with analog PET. J Nucl Med. 2015;56:1378–85.

32. Miller M, Zhang J, Binzel K, Griesmer J, Laurence T, Narayanan M,et al. Characterization of the Vereos Digital Photon Counting PET System. J Nucl Med. 2015;56:434.

33. van Sluis J, de Jong J, Schaar J, et al. Performance characteristics of the digital biograph vision PET/CT system. J Nucl Med. 2019;60:1031–6.

34. Lecomte R. Novel detector technology for clinical PET. Eur J Nucl Med Mol Imaging. 2009;36(Suppl 1):S69-85.

35. Del Guerra A, Belcari N, Bisogni MG, LLosa G, Marcatili S, Ambrosi G, et al. Advantages and pitfalls of the silicon photomultiplier (SiPM) as photodetector for the next generation of PET scanners. Nuclear Instruments and Methods in Physics Research Section A: Accelerators, Spectrometers, Detectors and Associated Equipment. 2010;617:223–226.

36. Karp JS, Surti S, Daube-Witherspoon ME, Muehllehner G. Benefit of time-of-flight in PET: experimental and clinical results. J Nucl Med. 2008;49:462–70.

37. Conti M. Focus on time-of-flight PET: the benefits of improved time resolution. Eur J Nucl Med Mol Imaging. 2011;38:1147–57.

38. Hsu DFC, Ilan E, Peterson WT, Uribe J, Lubberink M, Levin CS. Studies of a next-generation silicon-photomultiplier-based time-of-flight PET/CT system. J Nucl Med. 2017;58:1511–8.

39. Surti S, Karp JS. Advances in time-of-flight PET. Phys Med. 2016;32:12–22.

40. Zhang JMM, Knopp MV. Performance evaluation of digital PET/CT: medical physics basis for the clinical applications. Med Phys. 2016;43:3399.

41. Li X, Qi W, Miyahara M, Kolthammer J. Performance characterization of an SiPM-based time-of-flight Canon PET/CT scanner. J Nucl Med. 2020;61;

42.• Klein R, deKemp RA. Selection of PET camera and implications on the reliability and accuracy of absolute myocardial blood flow quantification. Curr Cardiol Rep. 2020;22:109. **This was a helpful review, from two years ago, on the different technical challenges withPET cameras and scanners, their potential solutions, and the resultant implications, forcardiovascular PET imaging, particularly MPI and quantification of MBF.**

43.• Van Dijk JD, Jager PL, Van Osch JAC, Khodaverdi M, Van Dalen JA. Comparison of maximal Rubidium-82 activities for myocardial blood flow quantification between digital and conventional PET systems. J Nucl Cardiol. 2019;26:1286–91. **This study offered a very interesting comparison between three different systems for PET-based MBF quantification. Two of them were conventional PET scanners and the third wasa digital PET scanner prototype.**

44. Levin C, Peterson W, Ross S, Stearns C, Uribe J. PET performance as a function of axial field of view for a new silicon photomultiplier-based whole body TOF PET/CT system. J Nucl Med. 2016;57.

45. Pan T, Einstein SA, Kappadath SC, et al. Performance evaluation of the 5-Ring GE Discovery MI PET/CT system using the national electrical manufacturers association NU 2–2012 Standard. Med Phys. 2019;46:3025–33.

46. Armstrong IS, Hayden C, Memmott MJ, Arumugam P. A preliminary evaluation of a high temporal resolution data-driven motion correction algorithm for rubidium-82 on a SiPM PET-CT system. J Nucl Cardiol. 2022;29:56–68.

47.•• Han Y, Ahmed AI, Hayden C, Jung AK, Saad JM, Spottiswoode B, et al. Change in positron emission tomography perfusion imaging quality with a data-driven motion correction algorithm. J Nucl Cardiol. 2022. **A novel data-driven motion correction algorithm was developed and evaluated forcardiac PET imaging. When compared to non-corrected images, the developed algorithm allowed an improvement in quality. Physician interpretation was correlated with machinemeasurement of motion quantification.**

48. DIETZ M, Kamani CH, Allenbach G, Rubimbura V, Fournier S, Lalonde MN, et al. Comparison of the prognostic value of global and regional myocardial flow capacity radius, myocardial flow reserve, and stress myocardial blood flow using Rubidium-82 with SiPM PET/CT. Preprint-Research Square. 2021.

49. DIETZ M, Kamani CH, Allenbach G, Rubimbura V, Fournier S, Lalonde MN, et al. Prognostic value of myocardial flow capacity and global absolute perfusion measurements using Rubidium-82 with SiPM PET/CT. Annual Congress of the European Association of Nuclear Medicine October 15–19. Barcelona, Spain. Eur J Nucl Med Mol Imaging. 2022;2022(49):S67-68.

50.•• Ahmed AI, Al Rifai M, Alahdab F, Saad JM, Han Y, Alfawara MS, et al. Incremental prognostic value of digital positron emission tomography derived myocardial flow reserve: a prospective cohort study. Int J Cardiol. 2022. **This study assessed the potential incremental prognostic prediction added by quantifyingMFR using digital PET scanners. The result was a significantly improved discriminationcoefficient using an MFR cutoff of 2 quantified by the digital PET machine.**

51. Lortie M, Beanlands RS, Yoshinaga K, Klein R, Dasilva JN, DeKemp RA. Quantification of myocardial blood flow with 82Rb dynamic PET imaging. Eur J Nucl Med Mol Imaging. 2007;34:1765–74.

Publisher's Note Springer Nature remains neutral with regard to jurisdictional claims in published maps and institutional affiliations.